Taxol Differentially Modulates the Dynamics of Microtubules Assembled from Unfractionated and Purified β-Tubulin Isotypes†

W. Brent Derry,‡ Leslie Wilson,‡ Israr A. Khan,§ Richard F. Ludueña,§ and Mary Ann Jordan*,‡

Department of Molecular, Cellular, and Developmental Biology and Neuroscience Research Institute, University of California, Santa Barbara, Santa Barbara, California 93106, and Department of Biochemistry, The University of Texas Health Science Center, 7703 Floyd Curl Drive, San Antonio, Texas 78284-7760

Received October 31, 1996; Revised Manuscript Received January 21, 1997⊗

ABSTRACT: Substoichiometric binding of taxol to tubulin in microtubules potently suppresses microtubule dynamics, which appears to be the most sensitive antiproliferative mechanism of taxol. To determine whether the β-tubulin isotype composition of a microtubule can modulate sensitivity to taxol, we measured the effects of substoichiometric ratios of taxol bound to tubulin in microtubules on the dynamics of microtubules composed of purified $\alpha\beta_{II}$-, $\alpha\beta_{III}$-, or $\alpha\beta_{IV}$-tubulin isotypes and compared the results with the effects of taxol on microtubules assembled from unfractionated tubulin. Substoichiometric ratios of bound taxol in microtubules assembled from purified β-tubulin isotypes or unfractionated tubulin potently suppressed the shortening rates and the lengths shortened per shortening event. Correlation of the suppression of the shortening rate with the stoichiometry of bound taxol revealed that microtubules composed of purified $\alpha\beta_{II}$-, $\alpha\beta_{III}$-, and $\alpha\beta_{IV}$-tubulin were, respectively, 1.6-, 7.4-, and 7.2-fold less sensitive to the effects of bound taxol than microtubules assembled from unfractionated tubulin. These results indicate that taxol differentially modulates microtubule dynamics depending upon the β-tubulin isotype composition. The results are consistent with recent studies correlating taxol resistance in tumor cells with increased levels of β_{III}- and β_{IV}-tubulin expression and suggest that altered cellular expression of β-tubulin isotypes can be an important mechanism by which tumor cells develop resistance to taxol.

Taxol is an important cancer chemotherapeutic agent for treatment of advanced ovarian and breast carcinoma, and it shows promising activity against several other carcinomas (Arbuck et al., 1994; Gelmon, 1994; Buzdar et al., 1995; Chang & Garrow, 1995; McGuire et al., 1996). It is a potent inhibitor of eukaryotic cell proliferation, blocking cell cycle progression at mitosis through its stabilizing actions on microtubules (Fuchs & Johnson, 1978; Schiff & Horwitz, 1980; Jordan et al., 1993).

Microtubules are long, hollow cylinders approximately 25 nm in diameter composed of dimeric subunits of α- and β-tubulin (Dustin, 1984). During microtubule assembly, the energy liberated by hydrolysis of tubulin-liganded guanosine 5′-triphosphate (GTP)[1] gives rise to a nonequilibrium behavior termed dynamic instability (Mitchison & Kirschner, 1984a,b). Dynamic instability is the stochastic interconversion of microtubule ends between phases of growth and shortening and is believed to arise from the gain and loss of a stabilizing cap of GTP or GDP−P_i on the terminal β-tubulin subunits (Mitchison & Kirschner, 1984b; Carlier, 1989).

Taxol binds reversibly to microtubules *in vitro* with a maximum stoichiometry of 1 mol of taxol per mol of tubulin in microtubules (Parness & Horwitz, 1981; Díaz et al., 1993) and an apparent dissociation constant in the 10 nM range [see Caplow et al. (1994)]. Taxol inhibits tubulin exchange at microtubule ends and treadmilling at polymer mass steady-state (Caplow & Zeeberg, 1982; Wilson et al., 1985). It exhibits differential effects on microtubule properties at different binding stoichiometries (Derry et al., 1995). Substoichiometric binding of taxol to tubulin in microtubules potently suppresses microtubule shortening rates but does not affect growing rates or polymer mass. However, at taxol concentrations that are stoichiometric or near-stoichiometric with respect to the concentration of tubulin in solution, dynamics are almost completely suppressed (Derry et al., 1995), and there is a strong stimulation of the rate and extent of microtubule polymerization *in vitro* (Schiff et al., 1979; Kumar, 1981; Howard & Timasheff, 1988; Derry et al., 1995) and *in vivo* (Schiff & Horwitz, 1980; De Brabander et al., 1981; Rowinski et al., 1988; Jordan et al., 1993).

Tubulins are encoded by small, heterogeneous multigene families in most organisms (Sullivan, 1988). Although neither regulatory nor structural multiplicity of tubulin genes has been demonstrated to be essential for cell growth or division, it is becoming clear that tubulin isotypes play critical roles in development, differentiation, and cell function (Hoyle & Raff, 1990; Matthews et al., 1993; Ludueña, 1993). The vertebrate β-tubulin gene family contains seven distinct

† This work was supported by USPHS Grant CA57291 from the National Cancer Institute (M.A.J. and L.W.), Grants GM23476 and CA26376 from the National Institutes of Health (R.F.L.), and Welch Foundation Grant AQ-0726 (R.F.L.), and was partially supported by the MRL Program of the National Sciences Foundation under Award DMR-9123048 (L.W. and W.B.D.).

* Corresponding author. Telephone: 805-983-3959. Fax: 805-893-4724.

‡ University of California, Santa Barbara.

§ The University of Texas Health Science Center.

⊗ Abstract published in *Advance ACS Abstracts,* March 1, 1997.

[1] Abbreviations: EGTA, [ethylenebis(oxyethylenenitrilo)]tetraacetic acid; GTP, guanosine 5′-triphosphate; MAPs, microtubule-associated proteins; MES, 2-(*N*-morpholino)ethanesulfonic acid; PEM, 100 mM PIPES, 1 mM EGTA, 1 mM $MgSO_4$, pH 6.9; PIPES, 1,4-piperazinediethanesulfonic acid; PMME, 86 mM PIPES, 36 mM MES, 1 mM EGTA, 1.4 mM $MgSO_4$, pH 6.8.

S0006-2960(96)02724-9 CCC: $14.00

genes, each of which encodes a structurally unique β-tubulin isotype [reviewed by Sullivan (1988)]. Different β-tubulin isotypes have been shown to coassemble into microtubules *in vivo* (Lewis et al., 1987; Lopata & Cleveland, 1987) and *in vitro* (Banerjee et al., 1988; Baker et al., 1990). Dimers containing purified β-tubulin isotypes assemble into microtubules at different critical concentrations *in vitro* (Banerjee et al., 1992) and possess differential binding affinities for the antimitotic agent colchicine (Banerjee & Ludueña, 1992). Purified, unfractionated bovine brain tubulin, which is composed of a mixture of different β-tubulin isotypes, has been determined to consist of 3% β_{I}-, 58% β_{II}-, 25% β_{III}-, and 13% β_{IV}-tubulin (Banerjee et al., 1988). Depletion of β_{III}-tubulin from unfractionated bovine brain tubulin results in increased microtubule assembly both in the absence and in the presence of taxol (Banerjee et al., 1990; Lu & Ludueña, 1993). Microtubules composed of purified β-tubulin isotypes display differential kinetics of growing and shortening under polymer mass steady-state conditions (Panda et al., 1994). Thus, regulation of the β-tubulin isotype composition may be one mechanism governing microtubule dynamics in cells.

Recent studies on mammalian cells selected for resistance to taxol have revealed that some resistant cells overexpress specific β-tubulin isotypes (Haber et al., 1995; Jaffrézou et al., 1995; Ranganathan et al., 1996) or contain altered electrophoretic variants of both α- and β-tubulin (Schibler & Cabral, 1986; Cabral & Barlow, 1989; Ohta et al., 1994). Overexpression of both β_{III}- and β_{IV}-tubulin has been reported in mammalian cell lines that are resistant to taxol (Jaffrézou et al., 1995; Ranganathan et al., 1996). These results suggest that altered expression of β-tubulin isotypes may lead to changes in cellular sensitivity to taxol.

In the present study, we found that microtubules composed of different αβ-tubulin isotypes require significantly different ratios of bound taxol to suppress their dynamics by similar magnitudes. The dynamics of microtubules assembled from purified $\alpha\beta_{III}$- or $\alpha\beta_{IV}$-tubulin were strikingly less sensitive to suppression by substoichiometric taxol binding than microtubules made from $\alpha\beta_{II}$-tubulin, unfractionated tubulin, or an equimolar ratio of $\alpha\beta_{II}$- and $\alpha\beta_{III}$-tubulin. The results suggest that the sensitivity of a tumor cell to taxol can be determined by the suppressive effects of bound taxol on microtubule dynamics, which in turn can be regulated by the β-tubulin isotype composition of the microtubules.

EXPERIMENTAL PROCEDURES

Purification of Bovine Brain Tubulin, αβ-Tubulin Isotypes and Axonemes. Bovine brain tubulin was purified from microtubule protein by phosphocellulose chromatography according to Fellous et al. (1977). Purified $\alpha\beta_{II}$-, $\alpha\beta_{III}$-, and $\alpha\beta_{IV}$-tubulin was prepared by immunoaffinity chromatography as described elsewhere (Banerjee et al., 1992; Khan & Ludueña, 1996) and stored at −70 °C in 100 mM MES, 1 mM EGTA, 0.1 mM EDTA, 0.5 mM $MgCl_2$, 8 M glycerol, and 1 mM GTP, pH 6.4. Immediately prior to use, glycerol was removed, and the isotypes were transferred to PMME buffer (86 mM PIPES, 36 mM MES, 1 mM EGTA, and 1.4 mM $MgSO_4$, pH 6.8; Panda et al., 1995) by passage through a Bio-Gel P-2 (Bio-Rad) column equilibrated with PMME buffer plus 0.1 mM GTP. Complete removal of glycerol was confirmed by adding ^{3}H-labeled glycerol to the sample prior to gel filtration (data not shown). The purity of the β-tubulin isotypes was estimated to be 95% for β_{II} (5% β_{I}), 86% for β_{III} (13% β_{II} + 1% β_{I}), and 100% for β_{IV} as determined by SDS−PAGE and quantitative immunoblot analysis. Although the α-tubulin isotype composition used in this work is not known, no differences have been reported in α-tubulin isotypes bound to different β-tubulin isotypes. Axonemal fragments, used to nucleate microtubules, were prepared from sea urchin sperm (*Lytechinus pictus*) according to Toso et al. (1993). Protein concentration was determined by the method of Bradford (1976) using bovine serum albumin as the standard.

Video Microscopy. Tubulin was mixed with axoneme seeds (~1×10^4 seeds/mL) and polymerized in PMME buffer containing 1 mM GTP in the presence or absence of taxol for 30 min at 37 °C. Polymer mass steady-state, estimated by turbidimetry at 350 nm, occurred <30 min after addition of nucleating axonemes as described in Derry et al. (1995). Because purified αβ-tubulin isotypes have distinct critical subunit concentrations (Banerjee et al., 1992), different concentrations of each αβ-tubulin isotype were required to assemble microtubules with similar lengths. Thus, the tubulin concentrations for all experiments were as follows: unfractionated tubulin, 16 μM; $\alpha\beta_{II}$, 10 μM; $\alpha\beta_{III}$, 7.0 μM; $\alpha\beta_{IV}$, 8.0 μM. The total tubulin concentration used to assemble microtubules from a 1:1 molar ratio of $\alpha\beta_{II}$- and $\alpha\beta_{III}$-tubulin was 12 μM. After assembly to polymer mass steady-state, growing and shortening dynamics of individual microtubules were recorded at 37 °C by differential interference contrast video microscopy as described by Derry et al. (1995). The "Video VanGogh" software package (a kind gift from Dr. E. D. Salmon, University of North Carolina, Chapel Hill) was used to measure microtubule length changes. Data points representing microtubule lengths were collected at 2−6 s intervals. Microtubules assembled predominantly at the plus ends of axonemal seeds under the conditions used, and plus ends were traced for an average duration of 10 min or until the microtubule underwent complete depolymerization. When microtubules assembled at both axonemal ends, plus-end microtubules were selected for measurement by their longer lengths and faster growing rates as compared with minus-end microtubules. Growing and shortening rates were calculated by least-squares regression analysis of the data points for each phase of growth or shortening. Shortening rates of control microtubules in this study are approximately 4 times greater than previously reported (Derry et al., 1995). The buffer conditions employed resulted in increased dynamics; in addition, refinements in the analysis method resulted in increased shortening rate values. A microtubule was considered to be in a growth phase if its length increased by >0.2 μm at a rate of >0.15 μm/min and in a shortening phase if its length decreased by >0.2 μm at a rate of >0.3 μm/min. Length changes equal to or less than 0.2 μm over the duration of six data points were considered attenuation (pause) phases. Between 24 and 36 microtubules from 3 to 5 separate experiments were measured for each condition. At taxol concentrations between 0 and 250 nM, the number of growing events ranged from 30 to 117, shortening events from 20 to 76, and attenuation events from 34 to 78.

Calculation of Transition Frequencies. The switching of a microtubule end from a phase of growth (or attenuation) to a phase of shortening is defined as a catastrophe, whereas the switching of a microtubule shortening event to a phase

of growth or attenuation is termed a rescue (Walker et al., 1988; Toso et al., 1993). The catastrophe frequency was calculated as the number of shortening events divided by the total time spent growing plus the total time spent in an attenuated state. The rescue frequency was calculated as the number of transition events from shortening to either growth or attenuation divided by the total time spent shortening. The number of rescues per micrometer was calculated by dividing the number of transitions from shortening to either growth or attenuation by the total length shortened (Kowalski & Williams, 1993). Percent polymer loss was calculated as the length of microtubule shortened divided by the microtubule length prior to the shortening event. The perturbation of shortening rate, as described previously (Gildersleeve et al., 1992), was analyzed over all taxol concentrations by dividing the number of shortening rate changes by the total number of shortening events. Dynamicity is defined as the total tubulin exchanged at a microtubule end during all detectable growing and shortening events divided by the total time of observation.

Determination of Microtubule Polymer Mass and Taxol Binding to Tubulin in Microtubules. Microtubule polymer mass and the stoichiometry of taxol bound to tubulin in microtubules were determined simultaneously by incubating tubulin in PMME buffer, diluted axoneme seeds ($\sim 1 \times 10^4$ seeds/mL), and 1 mM GTP (total solution volume 75 μL) for 30 min at 37 °C. Unlabeled taxol was mixed with [^{3}H]taxol (a kind gift from Dr. R. Haugwitz, National Cancer Institute, Research Triangle Park, NC) to obtain final concentrations of 25, 100, or 250 nM (specific activities: 1.5−15 Ci/mmol). Tubulin concentrations were identical to those used for video microscopy. Microtubules were sedimented in Beckman microfuge tubes (5 × 20 mm) using a prewarmed SW50.1 swinging-bucket rotor (150000*g*, 30 min, 37 °C, Beckman L5-50). Supernatants were carefully removed, and the concentration of unpolymerized tubulin was determined. Pelleted microtubules were gently washed with 75 μL of PMME buffer (37 °C) and then solubilized in 50 μL of 0.2 M NaOH. Microtubule protein in the pelleted fractions was quantitated, and bound taxol was determined by liquid scintillation counting. Taxol binding stoichiometry was expressed as the number of taxol molecules bound per molecule of tubulin dimer ($M_r = 100\,000$) in microtubules. Microtubule lengths were measured by video microscopy as described above.

RESULTS

Intrinsic Differences in the Dynamics of Isotypically Pure Microtubules in the Absence of Taxol. Control plus-end microtubules assembled to polymer mass steady-state from purified $\alpha\beta_{II}$-, $\alpha\beta_{III}$-, or $\alpha\beta_{IV}$-tubulin or unfractionated tubulin (Figure 1A,C,E,G) displayed episodes of relatively slow growth, rapid shortening, and phases of no detectable length change, termed attenuation, consistent with previous observations (Horio & Hotani, 1986; Walker et al., 1988; Gildersleeve et al., 1992; Pryer et al., 1992; Toso et al., 1993; Panda et al., 1994; Derry et al., 1995). Although all of the microtubules exhibited qualitatively similar dynamic instability behavior, as shown in Table 1, shortening rates, time in attenuation, and dynamicity differed among the microtubule isotypes quantitatively. The mean shortening rate of $\alpha\beta_{IV}$-microtubules (253 dimers s^{-1}) was significantly slower than the mean shortening rates of $\alpha\beta_{II}$- and $\alpha\beta_{III}$-microtubules

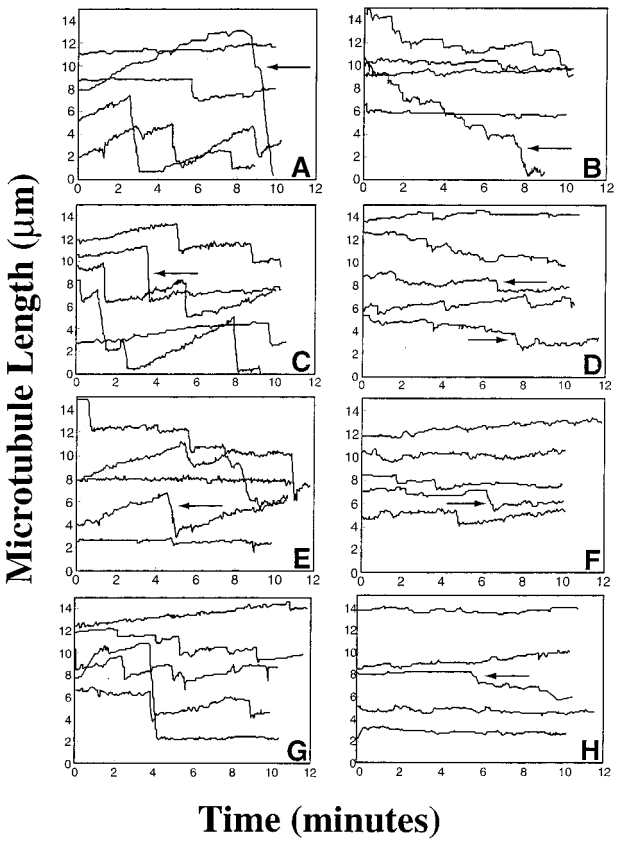

FIGURE 1: Growing and shortening at plus ends of individual microtubules composed of purified $\alpha\beta_{II}$- (A,B), $\alpha\beta_{III}$- (C, D), and $\alpha\beta_{IV}$-tubulin (E, F) and unfractionated tubulin (G, H) at steady-state in the absence or presence of taxol. Shown are life-history traces of untreated (control) microtubules (A, C, E, G) and microtubules in the presence of 250 nM taxol (B, D, F, H). Protein concentrations were 10, 7.0, 8.0, and 16 μM for $\alpha\beta_{II}$-, $\alpha\beta_{III}$-, and $\alpha\beta_{IV}$-tubulin and unfractionated tubulin, respectively. Each trace represents a single microtubule, and arrows show shortening rate changes within single shortening events.

(343 and 374 dimers s^{-1}, respectively; *t*-test: $p = 0.089$ for $\alpha\beta_{II}$- compared with $\alpha\beta_{IV}$-microtubules, $p = 0.025$ for $\alpha\beta_{IV}$-compared with $\alpha\beta_{III}$-microtubules). In addition, the mean shortening rate of microtubules assembled from unfractionated tubulin (684 dimers s^{-1}) was significantly higher than the mean shortening rates of microtubules made from any of the purified β-tubulin isotypes ($p < 0.003$ compared with all purified isotypes). There were no significant differences in the mean growing rates of microtubules made from any of the tubulin isotypes (Table 1).

Consistent with the results of Panda et al. (1994), $\alpha\beta_{III}$-microtubules were more dynamic than $\alpha\beta_{II}$- or $\alpha\beta_{IV}$-microtubules. For example, $\alpha\beta_{III}$-microtubules remained in an attenuated state only 23% of the time whereas $\alpha\beta_{II}$- and $\alpha\beta_{IV}$-microtubules remained in the attenuated state 44 and 42% of the time, respectively (Table 1). The dynamicity of $\alpha\beta_{II}$ - and $\alpha\beta_{IV}$-microtubules was 19 dimers s^{-1}, respectively, while microtubules made from purified $\alpha\beta_{III}$-tubulin and from unfractionated tubulin had relatively higher dynamicity values (33 and 26 dimers s^{-1}, respectively, Table 1).

Modulation by Taxol of the Dynamics of Microtubules Assembled from Pure β-Tubulin Isotypes and Unfractionated Tubulin. We determined the effects of taxol at a range of low concentrations (25−250 nM) on the dynamics of microtubules assembled from purified $\alpha\beta_{II}$-, $\alpha\beta_{III}$-, or $\alpha\beta_{IV}$-tubulin or unfractionated tubulin. Examination of micro-

Table 1: Effects of 250 nM Taxol on Dynamics of Microtubules Assembled from Purified $\alpha\beta_{II}$-, $\alpha\beta_{III}$-, or $\alpha\beta_{IV}$-Tubulin or Unfractionated Tubulin

	tubulin isotype							
	$\alpha\beta_{II}$		$\alpha\beta_{III}$		$\alpha\beta_{IV}$		unfractionated	
parameter	control	taxol	control	taxol	control	taxol	control	taxol
mean rate (dimers s^{-1})								
growing	14 ± 1[a]	17 ± 2	16 ± 1	17 ± 1	17 ± 2	16 ± 2	16 ± 1	16 ± 2
shortening	343 ± 45	147 ± 37	374 ± 44	132 ± 21	253 ± 34	116 ± 21	684 ± 113	45 ± 8
dynamicity	19 ± 3	11 ± 2	33 ± 6	19 ± 4	19 ± 3	11 ± 2	26 ± 5	7 ± 2
mean length per event (μm)								
growing	1.1 ± 0.2	0.5 ± 0.1	0.9 ± 0.03	0.5 ± 0.03	0.8 ± 0.1	0.5 ± 0.05	0.8 ± 0.1	0.5 ± 0.1
shortening	2.1 ± 0.4	0.8 ± 0.2	2.0 ± 0.4	0.6 ± 0.03	1.2 ± 0.1	0.6 ± 0.1	1.4 ± 0.2	0.4 ± 0.05
mean phase durations (s)								
growing	117 ± 10	57 ± 5	103 ± 7	64 ± 5	116 ± 9	83 ± 11	87 ± 7	66 ± 8
shortening	13 ± 2	15 ± 4	14 ± 2	17 ± 3	13 ± 2	19 ± 4	6 ± 1	22 ± 2
attenuation	187 ± 26	258 ± 29	95 ± 11	126 ± 13	143 ± 18	202 ± 24	163 ± 26	152 ± 23
% time								
growing	52 ± 6	16 ± 4	70 ± 16	37 ± 4	54 ± 6	21 ± 4	47 ± 6	21 ± 4
shortening	4 ± 4	6 ± 2	7 ± 1	10 ± 2	4 ± 1	6 ± 2	3 ± 1	9 ± 2
attenuation	44 ± 4	78 ± 5	23 ± 2	53 ± 4	42 ± 6	73 ± 5	50 ± 7	70 ± 4
no. of microtubules	35	30	31	25	31	27	28	13

[a] Errors are standard error of the mean.

tubule life-history traces in the absence and presence of 250 nM taxol indicated that the dynamics of microtubules of all isotype compositions were suppressed by the drug (Figure 1). To compare quantitatively the effects of taxol on microtubules assembled from each tubulin isotype, the kinetic parameters of dynamics were calculated (Table 1). Taxol suppressed the shortening rates, dynamicity, and mean length excursions per growing or shortening event of microtubules composed of purified β-tubulin isotypes and of microtubules made from unfractionated tubulin. These effects were accompanied by longer durations of the attenuation phase, an increased percentage of time the microtubules spent in attenuation, shorter growing phase durations, and a slightly reduced percentage of time spent growing. However, the attenuation phase duration of microtubules made from unfractionated tubulin was not affected by taxol concentrations $\leq$250 nM. Thus, taxol suppressed the dynamics of microtubules assembled from each β-tubulin isotype examined by modulating similar dynamic parameters, but the degree to which the parameters were affected showed variability among the isotypes.

Stoichiometries of Taxol Bound to Tubulin in Microtubules The stoichiometries of taxol bound to tubulin in microtubules assembled from purified $\alpha\beta_{II}$-, $\alpha\beta_{III}$-, or $\alpha\beta_{IV}$-tubulin or unfractionated tubulin (Table 2) were determined as described under Experimental Procedures. Greater than 90% of the total taxol added was bound to microtubules at each drug concentration. The steady-state polymer mass levels of microtubules made from $\alpha\beta_{II}$-, $\alpha\beta_{III}$-, or $\alpha\beta_{IV}$-tubulin or unfractionated tubulin varied greatly in the absence of taxol (4.1, 3.6, 1.5, and 11 μM, respectively). Therefore, differences in taxol binding stoichiometries among microtubules assembled from distinct $\alpha\beta$-tubulin isotypes were attributable to the different polymer mass levels for each isotype. Microtubules made from purified $\alpha\beta_{II}$-tubulin or unfractionated tubulin had lower ratios of bound taxol than $\alpha\beta_{III}$- or $\alpha\beta_{IV}$-microtubules. For example, at 25 nM taxol, microtubules assembled from purified $\alpha\beta_{II}$-tubulin or unfractionated tubulin had 2 or 3 taxol molecules bound for every 1000 tubulin dimers, respectively, whereas $\alpha\beta_{III}$- and $\alpha\beta_{IV}$-microtubules had 4.4 and 12 taxol molecules bound for every 1000 dimers of tubulin in microtubules, respectively. Microtubules assembled from a 1:1 ratio of $\alpha\beta_{II}$- and $\alpha\beta_{III}$-tubulin had stoichiometries similar to those determined for purified $\alpha\beta_{II}$-microtubules.

Table 2: Stoichiometries of Taxol Bound to Tubulin in Microtubules Assembled from $\alpha\beta_{II}$-, $\alpha\beta_{III}$-, or $\alpha\beta_{IV}$-Tubulin or Unfractionated Tubulin[a]

	mol of bound taxol/1000 mol of tubulin in microtubules[a]		
tubulin isotype	25 nM taxol	100 nM taxol	250 nM taxol
$\alpha\beta_{II}$	2.0 ± 0.3	9.2 ± 1.5	21 ± 3
$\alpha\beta_{III}$	4.4 ± 2	24 ± 3	66 ± 17
$\alpha\beta_{IV}$	12 ± 3	51 ± 10	76 ± 10
unfractionated	3.0 ± 1.2	5.4 ± 8	15 ± 1
$\alpha\beta_{II}$:$\alpha\beta_{III}$ (1:1)	2.0 ± 3	9.3 ± 2	nd[c]

[a] Differences in the taxol binding stoichiometries among microtubules assembled from distinct β-tubulin isotypes are attributable to the variation in polymer mass levels (see Results) since greater than 90% of the taxol is bound at each drug concentration. [b] Stoichiometry of taxol bound to tubulin dimer (M_r = 100 000) in microtubules was determined as described under Experimental Procedures. [c] nd = not determined.

Effects of Taxol on Microtubule Shortening Events. To more clearly understand the differential effects of taxol on the dynamics of microtubules made from distinct β-tubulin isotypes, the stoichiometry of taxol bound to tubulin in microtubules was related to the magnitude by which the shortening rates were suppressed (Figure 2A). Microtubules composed of purified $\alpha\beta_{III}$- or $\alpha\beta_{IV}$-tubulin required higher ratios of bound taxol to suppress shortening rates (Figure 2A) and the mean lengths shortened (Figure 2B) than microtubules assembled from purified $\alpha\beta_{II}$-tubulin or unfractionated tubulin. For example, the mean shortening rate of $\alpha\beta_{II}$-microtubules was suppressed by 57% with 21 taxol molecules bound for every 1000 dimers of tubulin in the microtubules (Tables 1 and 2). In contrast, 76 taxol molecules bound per 1000 tubulin dimers were required to similarly suppress the mean shortening rate of $\alpha\beta_{IV}$-microtubules (by 54%). Thus, 3.6 times more bound taxol was necessary to suppress the mean shortening rate of $\alpha\beta_{IV}$-microtubules to the same extent as $\alpha\beta_{II}$-microtubules.

Perturbation of Shortening by Taxol. Single shortening events often displayed one or more rate changes as a

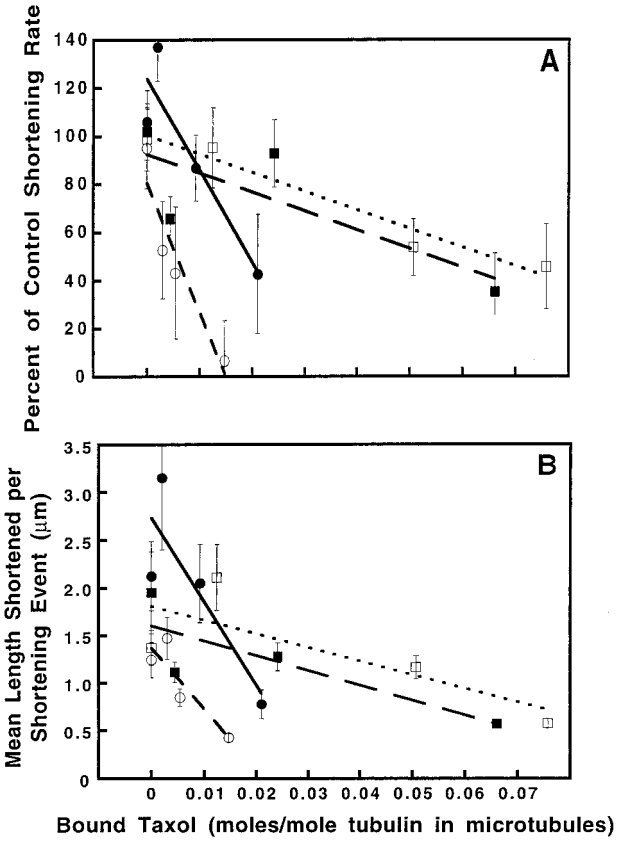

FIGURE 2: Effects of taxol bound to tubulin in microtubules on percent suppression of mean shortening rates relative to untreated controls (A), and mean length shortened during shortening events (B) for microtubules assembled from purified $\alpha\beta_{II}$- (●, solid line), $\alpha\beta_{III}$- (■, long dashed line), or $\alpha\beta_{IV}$-tubulin (□, dotted line), and unfractionated tubulin (○, short dashed line). Data points are the mean ± SEM. Lines are linear regressions. Data points in the absence of taxol have been offset slightly in panel A.

microtubule disassembled (arrows in Figure 1), a behavior described previously with microtubules made from unfractionated bovine brain tubulin (O'Brien et al., 1990; Gildersleeve et al., 1992). Microtubules assembled from purified $\alpha\beta_{II}$-, $\alpha\beta_{III}$-, and $\alpha\beta_{IV}$-tubulin changed shortening rates with a frequency of 0.06−0.08 times per shortening event, whereas the frequency of changes in shortening rate was 0.19 times per shortening event for microtubules made from unfractionated tubulin. The frequency of shortening rate changes increased in a taxol concentration-dependent manner for $\alpha\beta_{II}$-, $\alpha\beta_{III}$-, and $\alpha\beta_{IV}$-microtubules to frequencies of 0.52, 0.18, and 0.27, respectively, at 250 nM taxol, but was not affected in microtubules assembled from unfractionated tubulin (data not shown).

Effects of Taxol on the Percent Time in an Attenuated State and on the Transition Frequencies. Taxol increased the percentage of time that microtubules of all β-tubulin isotype compositions spent in an attenuated state (Figure 3). Similar to the suppressive effect of taxol on shortening, a higher ratio of bound taxol was required to increase the percentage of time in an attenuated state with $\alpha\beta_{III}$- or $\alpha\beta_{IV}$-microtubules than microtubules assembled from purified $\alpha\beta_{II}$-tubulin or unfractionated tubulin.

Unlike the potent effects of taxol on microtubule shortening rates and lengths shortened during a shortening event, the frequency of catastrophe (transitions to shortening from phases of growth or attenuation) was largely unaffected over

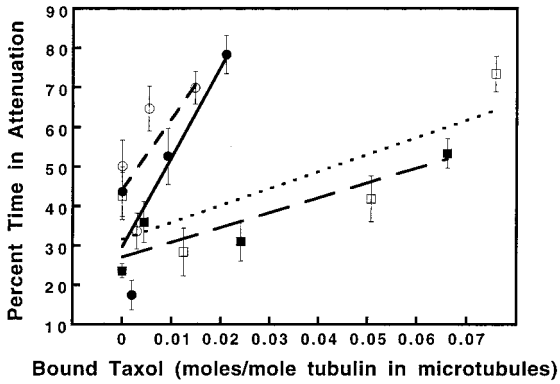

FIGURE 3: Relationship between percentage of time microtubules spent in an attenuated state of dynamic activity and the stoichiometry of taxol bound to tubulin in microtubules assembled from $\alpha\beta_{II}$- (●, solid line), $\alpha\beta_{III}$- (■, long dashed line), and $\alpha\beta_{IV}$-tubulin (□, dotted line), and unfractionated tubulin (○, short dashed line). Data points are the mean ± SEM. Lines are linear regressions.

the taxol concentration range examined (Table 3). Rescue frequency relative to microtubule length shortened increased in a taxol concentration-dependent manner (Figure 4), but rescue frequency relative to time spent shortening decreased (Table 3). This apparent discrepancy is resolved when one considers the fact that as microtubules spend longer durations of time in the shortening phase at low taxol concentrations their time-dependent rescue frequencies decrease (Table 1 and see below). Rescue frequency based on length shortened (Figure 4) increased because microtubules underwent shorter length excursions per shortening event in the presence of taxol.

Effects of Bound Taxol on Polymer Mass and Microtubule Lengths. The polymer mass and mean lengths of microtubules assembled from purified $\alpha\beta$-tubulin isotypes (Figure 5) increased substantially at lower taxol binding stoichiometries than were required to detectably suppress shortening rates and lengths shortened per shortening event (Figure 2). For example, $\alpha\beta_{II}$-microtubules showed a 2-fold increase in polymer mass and an increase in mean microtubule length from 5 to 12 μm at very low stoichiometries of taxol bound to tubulin in the microtubules (9.2 taxol molecules bound per 1000 $\alpha\beta_{II}$-tubulin subunits in microtubules, Figure 5A). However, the mean length and polymer mass of microtubules made from unfractionated tubulin remained unchanged at taxol concentrations which potently suppressed shortening rates and lengths shortened (Figure 5D), consistent with our previous observations (Derry et al., 1995).

Modulation of the Dynamics of Microtubules Assembled from a 1:1 Mixture of $\alpha\beta_{II}$- and $\alpha\beta_{III}$-Tubulin. To compare the effects of taxol on the modulation of the dynamics of microtubules made from two different β-tubulin isotypes, a 1:1 mixture of $\alpha\beta_{II}$- and $\alpha\beta_{III}$-tubulin (final tubulin concentration 12 μM) was assembled to polymer mass steady-state, and the dynamic parameters of the resulting microtubules were analyzed (Table 4). In the absence of taxol, these isotypically-mixed microtubules underwent shorter length excursions and were more attenuated than microtubules composed of either purified isotype alone; however, their mean shortening rate was not significantly different from those of microtubules assembled from either purified isotype alone (Table 1). Interestingly, the dynamicity of the isotypically-mixed microtubules was 26 dimers s^{-1}, which is exactly the mean of dynamicity values calculated for $\alpha\beta_{II}$-

Table 3: Effects of Taxol on Transition Events per Unit Time of Microtubules Assembled to Polymer Mass Steady-State from Purified β-Tubulin Isotypes or Unfractionated Tubulin

	catastrophe frequency (min^{-1})				rescue frequency (min^{-1})			
tubulin isotype	control	25 nM taxol	100 nM taxol	250 nM taxol	control	25 nM taxol	100 nM taxol	250 nM taxol
$\alpha\beta_{II}$	0.18 ± 0.03	0.22 ± 0.04	0.20 ± 0.04	0.15 ± 0.03	3.2 ± 0.5	3.1 ± 0.6	2.7 ± 0.6	2.4 ± 0.4
$\alpha\beta_{III}$	0.27 ± 0.04	0.24 ± 0.04	0.24 ± 0.04	0.31 ± 0.06	4.0 ± 0.7	4.4 ± 0.8	4.7 ± 0.9	3.0 ± 0.6
$\alpha\beta_{IV}$	0.18 ± 0.03	0.11 ± 0.02	0.22 ± 0.04	0.18 ± 0.03	4.3 ± 0.8	3.0 ± 0.5	2.5 ± 0.4	2.7 ± 0.5
unfractionated	0.22 ± 0.04	0.21 ± 0.04	0.26 ± 0.04	0.24 ± 0.06	7.7 ± 1.4	3.5 ± 0.6	3.2 ± 0.5	2.3 ± 0.6

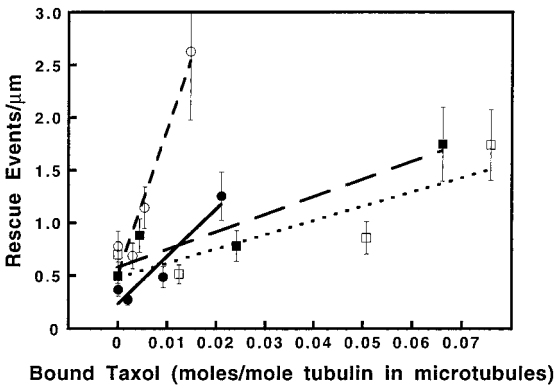

FIGURE 4: Effects of bound taxol on the rescue frequency per micrometer of length shortened for purified $\alpha\beta_{II}$- (●, solid line), $\alpha\beta_{III}$- (■, long dashed line), and $\alpha\beta_{IV}$-tubulin (□, dotted line), and unfractionated tubulin (○, short dashed line). Rescue frequencies were calculated by dividing the total number of rescues by the total shortening lengths for all microtubules. Data points are the mean ± SEM. Lines are linear regressions.

and $\alpha\beta_{III}$-microtubules (19 and 33 dimers s^{-1}, respectively; Tables 1 and 4).

The dynamics of microtubules assembled from a 1:1 mixture of $\alpha\beta_{II}$- and $\alpha\beta_{III}$-tubulin were more sensitive to the suppressive effects of taxol than microtubules composed of either purified isotype alone. For example, at 100 nM taxol (*i.e.*, bound taxol:tubulin stoichiometry of 9.3:1000, Table 2), the mean shortening rate of the isotypically-mixed microtubules was suppressed by 47%, and the mean length shortened per shortening event was suppressed by 56% (Table 4). However, at 100 nM taxol, the mean shortening rates of microtubules composed of purified $\alpha\beta_{II}$- or $\alpha\beta_{III}$-tubulin were suppressed by only 13% or 7%, respectively, at taxol:tubulin stoichiometries of 9.2:1000 and 24:1000, respectively (Figure 2A). Taxol did not remarkably affect growing events of microtubules assembled from a 1:1 mixture of $\alpha\beta_{II}$- and $\alpha\beta_{III}$-tubulin except that the mean growing rate and the length grown per growing event decreased slightly at 100 nM taxol.

DISCUSSION

Microtubules composed of purified $\alpha\beta_{III}$- and $\alpha\beta_{IV}$-tubulin were strikingly less sensitive to the suppressive effects of bound taxol than microtubules assembled from $\alpha\beta_{II}$-tubulin, an equal ratio of $\alpha\beta_{II}$- and $\alpha\beta_{III}$-tubulin, or unfractionated tubulin. As with microtubules assembled from unfractionated tubulin (Derry et al., 1995), the most potent effect of taxol on the dynamics of isotypically-purified microtubules was the selective suppression of shortening rates and lengths shortened (Figure 2).

Correlation of Suppressive Effects of Taxol with Binding Stoichiometries: "Suppressivity". The effects of taxol on the dynamic instability parameters of microtubules were related to the stoichiometry of taxol bound to tubulin in the microtubules rather than to the total concentration of drug added because purified $\alpha\beta$-tubulin isotypes assemble into microtubules with different critical concentrations (Banerjee et al., 1992). The suppression of shortening rates as a function of bound taxol is shown in Figure 2A. The slopes of the linear regression lines represent the efficacy of bound taxol in suppressing shortening rates (Table 5), a parameter we call "suppressivity" or the coefficient of suppression (*Sp*). From the equation of a straight line:

$$y = (Sp)x + b \quad (1)$$

where y = the shortening rate, Sp = suppressivity, x = the stoichiometry of bound taxol, and b = the shortening rate in the absence of taxol, the suppressivity $Sp = |(y - b)/x|$. Taxol suppressivities of the mean shortening rate for microtubules assembled from each $\alpha\beta$-tubulin isotype ranked in order of decreasing sensitivity to bound taxol were as follows: unfractionated > $\alpha\beta_{II}$- > $\alpha\beta_{III}$- = $\alpha\beta_{IV}$-tubulin (Table 5). Suppressivity may be applied to any kinetic parameter of microtubule dynamics that is altered by the binding of a modulating molecule (*e.g.*, drugs, MAPs).

The relative magnitude of taxol suppressivity for microtubules composed of each purified $\alpha\beta$-tubulin isotype is expressed by the ratio $Sp_{PC}/Sp_{\alpha\beta}$, where Sp_{PC} is the suppressivity value for microtubules made from unfractionated tubulin and $Sp_{\alpha\beta}$ is the suppressivity value for microtubules of a particular $\alpha\beta$-tubulin isotype composition. Thus, $\alpha\beta_{III}$- and $\alpha\beta_{IV}$-microtubules were, respectively, 7.4 and 7.2 times less sensitive than unfractionated microtubules to the suppression of shortening rates by taxol binding, whereas $\alpha\beta_{II}$-microtubules were only 1.6 times less sensitive than unfractionated microtubules (Table 5). Using this same approach to distinguish degrees of microtubule stability based on the percentage of time spent in the attenuated state, a parallel relationship among microtubule isotype classes emerged (Table 5).

The binding affinities of taxol for isotypically purified microtubules were not determined since almost all of the taxol was bound to the microtubules over the range of drug concentrations examined. Cellular taxol concentrations are often far above the apparent k_D value for microtubules (Jordan et al., 1993, 1996; Caplow et al., 1994); thus, differences in binding affinities may not be as important for the regulation of microtubule dynamics by taxol as the conformational changes induced in a particular isotype by bound taxol. In summary, the data indicate that the sensitivity of microtubule dynamics to bound taxol can be regulated by the β-tubulin isotype composition, and suggest that incorporation of appreciable quantities of $\alpha\beta_{III}$- and $\alpha\beta_{IV}$-tubulin into microtubules might significantly reduce the efficacy of taxol.

Mechanistic Implications. Microtubules assembled from mixtures of $\alpha\beta$-tubulin isotypes displayed dynamic properties

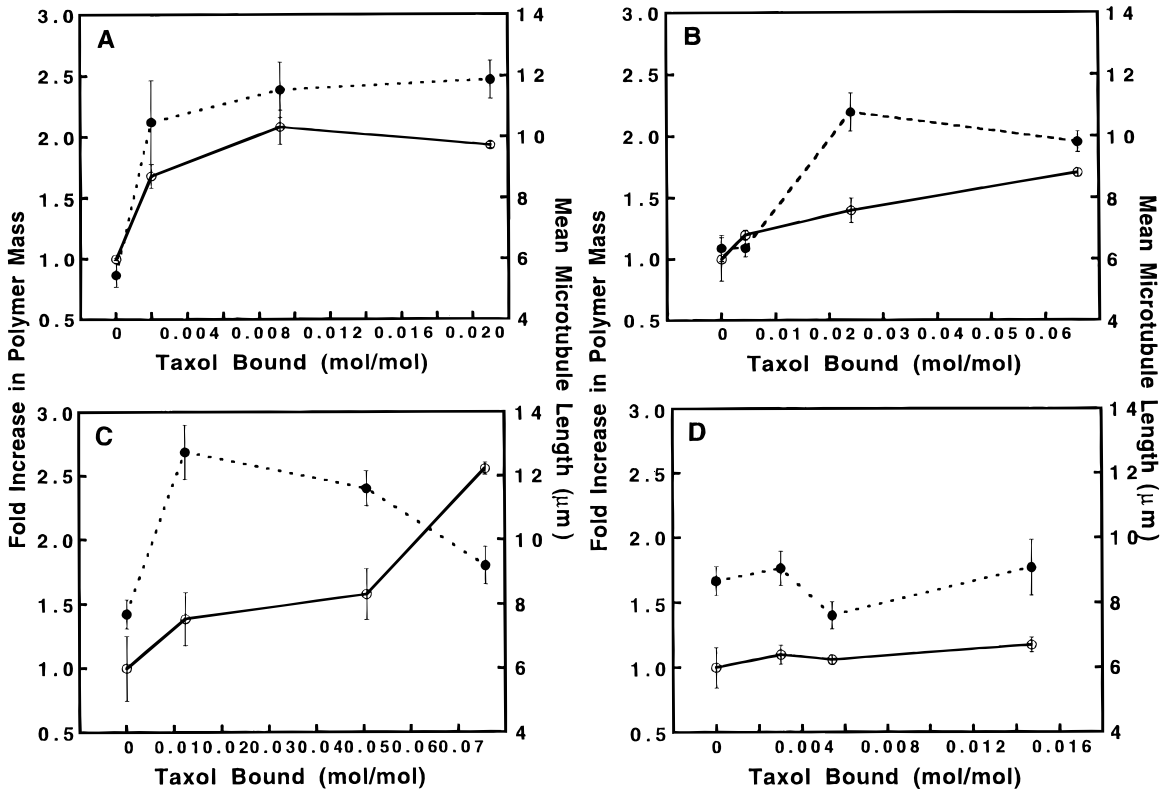

FIGURE 5: Effects of bound taxol on polymer mass (○) relative to controls determined by sedimentation (Experimental Procedures) and mean lengths of microtubules (●) assembled from $\alpha\beta_{II}$- (A), $\alpha\beta_{III}$- (B), and $\alpha\beta_{IV}$-tubulin (C) and unfractionated tubulin (D). Protein concentrations were the same as noted in Figure 1. Data points are the mean ± SEM.

Table 4: Effects of Taxol on Dynamics of Microtubules Assembled from a 1:1 Mixture of $\alpha\beta_{II}$- and $\alpha\beta_{III}$-Tubulin

	taxol concn (nM)		
parameter	0	25	100
mean rate (dimers s^{-1})			
growing	20.6 ± 2.1	23.0 ± 2.3	16.6 ± 1.2
shortening	423.9 ± 63.4	318.5 ± 48.0	223.8 ± 48.8
dynamicity	26.0	30.4	14.5
mean length per event (μm)			
grown	0.72 ± 0.05	0.89 ± 0.05	0.57 ± 0.02
shortened	1.29 ± 0.14	1.01 ± 0.12	0.57 ± 0.04
% time			
growing	16.7	45.8	22.5
shortening	5.3	6.2	4.8
attenuation	78.0	48.0	72.7
transition events			
catastrophe frequency (min^{-1})	0.23	0.30	0.28
rescue frequency (min^{-1})	4.1	4.5	5.6
polymer loss per shortening event (%)	25.8 ± 3.1	13.1 ± 1.8	6.2 ± 0.5
microtubule length (μm)	6.52 ± 0.30	9.78 ± 0.52	9.47 ± 0.34
no. of microtubules obsd	37	25	23

[a] Errors are standard error of the mean.

that were not always predictable from their behaviors as purified polymers. For example, the mean shortening rate of microtubules composed of unfractionated tubulin was 684 dimers s^{-1}, while $\alpha\beta_{II}$-, $\alpha\beta_{III}$-, and $\alpha\beta_{IV}$-microtubules disassembled at mean rates of 343, 374, and 253 dimers s^{-1}, respectively (Table 1). The significantly higher mean shortening rate of microtubules assembled from unfractionated tubulin indicates that the mechanism of microtubule disassembly may be determined in a complex manner by the tubulin isotype composition. The heterogeneity of unfractionated tubulin may create a heterogeneous microtubule structure with differences in the physical contacts (*i.e.*, attractive forces) between tubulin subunits, which could influence the kinetics of assembly and disassembly. In other words, a microtubule composed of several different $\alpha\beta$-tubulin isotypes might sample through more kinetic pathways as it grows or shortens than microtubules made from a single tubulin isotype. Such heterogeneity might also underlie the higher frequency of shortening rate changes observed with control microtubules assembled from unfractionated tubulin compared with those made of purified β-tubulin isotypes.

Microtubules assembled from purified $\alpha\beta_{II}$-tubulin were more sensitive to suppression of shortening and changes in polymer mass by taxol binding than microtubules composed of purified $\alpha\beta_{III}$- or $\alpha\beta_{IV}$-tubulin. For example, maximal incorporation of tubulin into microtubules made from purified

Table 5: Taxol Suppressivity and *S!* Values for Microtubules Composed of $\alpha\beta$-Tubulin Isotypes or Unfractionated Tubulin

tubulin isotype	shortening rate suppressivity[a]	r[d]	*S!*[c] (shortening rate)	attenuation suppressivity[b]	r	*S*! (attenuation)
$\alpha\beta_{II}$	3626	0.884	1.6	2281	0.863	0.8
$\alpha\beta_{III}$	765	0.785	7.4	377	0.899	4.7
$\alpha\beta_{IV}$	784	0.980	7.2	433	0.789	4.1
unfractionated	5639	0.931	1.0	1789	0.699	1.0

[a] Suppressivity values (*Sp*) based on shortening rates are the absolute values of slopes correlating percent suppression of shortening rates with stoichiometry of taxol bound (Figure 2A). [b] Suppressivity values (*Sp*) based on attenuation were determined from the slopes of lines correlating the percentage of time in attenuation with stoichiometry of taxol bound (Figure 3). [c] *S!* was calculated by dividing the *Sp* value for microtubules made from unfractionated tubulin by the *Sp* value for microtubules composed of the indicated purified $\alpha\beta$-tubulin isotype (see Discussion). [d] r = correlation coefficient of linear regression used to determine suppressivity.

$\alpha\beta_{II}$-tubulin occurred when 1 taxol molecule was bound for every 109 molecules of tubulin in microtubules, whereas microtubules composed of purified $\alpha\beta_{III}$-tubulin required 1 taxol for every 41 molecules of tubulin in microtubules. Howard and Timasheff (1988) have suggested that taxol lowers the linkage free energy of microtubule polymerization by strengthening lateral interactions between tubulin subunits. Low-resolution X-ray scattering studies confirmed that taxol induces changes in the lateral contact angle between protofilaments in microtubules (Andreu et al., 1992). We suggest that taxol binding lowers the free energy linking the incorporation of $\alpha\beta_{II}$-tubulin into microtubules more effectively than with microtubules assembled from purified $\alpha\beta_{III}$- or $\alpha\beta_{IV}$-tubulin or from unfractionated tubulin. This is consistent with the results of Lu and Ludueña (1993), who found that taxol more effectively promotes the assembly of microtubules from unfractionated tubulin depleted of $\alpha\beta_{III}$-tubulin. Similarily, Lobert et al. (1995) found a difference in the abilities of unfractionated and purified $\alpha\beta_{III}$-tubulin to associate into taxol-stabilized microtubules.

The polymer mass levels of microtubules assembled from unfractionated tubulin were not affected at taxol binding stoichiometries that potently suppressed their shortening rates. This relationship results from the taxol-induced increase in shortening phase duration and in percentage of time in shortening combined with the decrease in shortening rate (Table 1). These microtubules underwent catastrophes as often controls, but the presence of taxol molecules along their surfaces suppressed the off rate. Mechanistically, one could consider this as a battle between the energetics of stabilization by taxol binding and the energetics of disassembly intrinsic to the microtubule lattice. There was enough free energy in the lattice of microtubules made from unfractionated tubulin to drive disassembly through a region with taxol bound at low stoichiometry, albeit at a much slower rate. The suppressive effects of substoichiometric binding of taxol on microtubule shortening events were uncoupled from its effects on polymer mass.

The free energy change associated with taxol binding to tubulin might not be directly proportional to stabilization of the polymer, since one of the key regions likely to regulate polymer dynamics and stability is the divergent C-terminus of β-tubulin (Panda et al., 1994), which has not been shown to directly interact with taxol. Two putative sites of molecular contact for taxol have been identified near the N-terminal 31 amino acids and between amino acids 217 and 231 of β-tubulin (Rao et al., 1994, 1995). These regions show a high degree of sequence conservation between isotypes, although amino acids 31−40 display some variations (Sullivan, 1988). It is not known whether these regions of the β-tubulin molecule contribute to the regulation of microtubule dynamics.

Regulation of Taxol Sensitivity in Cells by the Tubulin Isotype Composition. Drug resistance presents one of the most difficult obstacles in the chemotherapeutic treatment of cancer. Many taxol-resistant mammalian cell lines have been isolated that have a variety of genetic lesions such as overexpression of the 170 kDa multidrug resistance protein (Gupta, 1983; Roy & Horwitz, 1985; Bhalla et al., 1994), electrophoretic alterations in α- and β-tubulin (Cabral et al., 1981; Schibler & Cabral, 1986; Ohta et al., 1994), and decreased levels of polymerized tubulin (Minotti et al., 1991). Recent studies have suggested that β-tubulin isotype levels may play an important role in resistance to antimitotic drugs. Jaffrézou et al. (1995) isolated a taxol-resistant human erythroleukemic cell line which overexpresses β_{IV}-tubulin by 200% and displays no multidrug resistance phenotype. Ranganathan et al. (1996) found that β_{III}- and β_{IV}-tubulin isotypes are overexpressed in a human prostate carcinoma cell line resistant to estramustine and taxol.

The correlation of β_{III}- and β_{IV}-tubulin overexpression with resistance to taxol agrees well with our results that $\alpha\beta_{III}$-microtubules and $\alpha\beta_{IV}$-microtubules are less sensitive to kinetic suppression of microtubule dynamics than microtubules assembled from purified $\alpha\beta_{II}$-tubulin, unfractionated tubulin, or a 1:1 mixture of $\alpha\beta_{II}$- and $\alpha\beta_{III}$-tubulin. In contrast, Haber et al. (1995) found that taxol-resistant murine cells overexpress β_{II}-tubulin 21-fold. However, these cells also overexpress the multidrug resistance P-glycoprotein. Taken together, these studies indicate that cells can modulate their sensitivity to taxol by altering levels of β-tubulin isotypes. Changes in tumor sensitivity by alteration of β-tubulin isotype expression may alter the efficacy of taxol administered clinically at levels which are often near the maximal tolerated dose of a narrow therapeutic concentration window.

Suppression of microtubule dynamics in cells by diverse antimitotic drugs such as vinblastine and taxol (Dhamodharan et al., 1995; A.-M. Yvon, P. Wadsworth, L. Wilson, and M. A. Jordan, unpublished results) has been shown to result in inhibition of cell proliferation and apoptotic cell death (Jordan et al., 1991, 1993, 1996). Thus, the effects of antimitotic agents on the dynamics of microtubules of distinct tubulin isotype compositions may predict drug efficacy in tumors with specific levels of tubulin isotypes.

ACKNOWLEDGMENT

We are grateful to Dr. Jacob Israelachvili and Dr. Joyce Wong of the Department of Chemical Engineering (UCSB)

for insightful discussions, and to James Flynn, Etsuko Tsuchiya, Dr. Dulal Panda, and Dr. Richard Himes for critical comments on the manuscript.

REFERENCES

Andreu, J. M., Bordas, J., Díaz, J. F., Garcia de Ancos, J., Gil, R., Medrano, F. J., Nogales, E., Pantos, E., & Towns-Andrews, E. (1992). *J. Mol. Biol. 226*, 169−184.

Arbuck, S. G., Dorr, A., & Friedman, M. A. (1994) *Hematol. Oncol. Clin. N. Am. 8*, 121−140.

Arnal, I., & Wade, R. H. (1995) *Curr. Biol. 5*, 900−908.

Baker, H. N., Rothwell, S. W., Grasser, W. A., Wallis, K. T., & Murphy, D. B. (1990) *J. Cell Biol. 110*, 97−104.

Banerjee, A., & Ludueña, R. F. (1992) *J. Biol. Chem. 267*, 13335−13339.

Banerjee, A., Roach, M. C., Wall, K. A., Lopata, M. A., Cleveland, D. W., & Ludueña, R. F. (1988) *J. Biol. Chem. 263*, 3029−3034.

Banerjee, A., Roach, M. C., Trcka, P., & Ludueña, R. F. (1990) *J. Biol. Chem. 265*, 1794−1799.

Banerjee, A., Roach, M. C., Trcka, P., & Ludueña, R. F. (1992) *J. Biol. Chem. 267*, 5625−5630.

Bhalla, K., Huang, Y., Tang, C., Self, S., Ray, S., Mahoney, M. E., Ponnathpur, V., Tourkina, E., Ibrado, A. M., Bullock, G., & Willingham, M. C. (1994) *Leukemia, 8*, 465−475.

Bradford, M. M. (1976) *Anal. Biochem. 72*, 248−254.

Buzdar, A. U., Holmes, F. A., & Hortobagyi, G. N. (1995) *Semin. Oncol. 22 (Suppl. 6)*, 101−104.

Cabral, F. R., & Barlow, S. B. (1989) *FASEB J. 3*, 1593−1599.

Cabral, F., Abraham, I., & Gottesman, M. M. (1981) *Proc. Natl. Acad. Sci. U.S.A. 78*, 4388−4391.

Caplow, M., & Zeeburg, B. (1982) *Eur. J. Biochem. 127*, 319−324.

Caplow, M., Shanks, J., & Ruhlen, R. (1994) *J. Biol. Chem. 269*, 23399−23402.

Carlier, M. F. (1989) *Int. Rev. Cytol. 115*, 139−170.

Chang, A. Y., & Garrow, G. C. (1995) *Semin. Oncol. 22 (Suppl. 6)*, 66−71.

DeBrabander, M., Geuens, G., Nuydens, R., Willebrords, R., & DeMey, J. (1981) *Proc. Natl. Acad. Sci. U.S.A, 78*, 5608−5612.

Derry, W. B., Wilson, L., & Jordan, M. A. (1995) *Biochemistry 34*, 2203−2213.

Dhamodharan, R., Jordan, M. A., Thrower, D., Wilson, L., & Wadsworth, P. (1995) *Mol. Biol. Cell 6*, 1215−1229.

Díaz, J. F., & Andreu, J. M. (1993) *Biochemistry 32*, 2747−2755.

Díaz, J. F., Menéndez, M., & Andreu, J. M. (1993) *Biochemistry 32*, 10067−10077.

Dustin, P. (1984) *Microtubules*, Springer-Verlag, Berlin.

Fellous, A., Francon, J., Lennon, A.-M., & Nunez, J. (1977) *Eur. J. Biochem. 78*, 167−174.

Fuchs, D. A., & Johnson, R. K. (1978) *Cancer Treat. Rep. 62*, 1219−1222.

Gelmon, K. (1994) *Lancet 344*, 1267−1272.

Gildersleeve, R. F., Cross, A. R., Cullen, K. E., Fagan, L. P., & Williams, R. C., Jr. (1992) *J. Biol. Chem. 267*, 7995−8006.

Gupta, R. S. (1983) *J. Cell. Physiol. 114*, 137−144.

Haber, M., Burkhart, C. A., Regl, D. L., Madafiglio, J., Norris, M. D., & Horwitz, S. B. (1995) *J. Biol. Chem. 270*, 31269−31275.

Horio, T., & Hotani, H. (1986) *Nature 321*, 605−607.

Howard, W. D., & Timasheff, S. N. (1988) *J. Biol. Chem. 263*, 1342−1346.

Hoyle, H. D., & Raff, E. C. (1990) *J. Cell Biol. 111*, 1009−1026.

Jaffrézou, J. P., Dumontet, C., Derry, W. B., Durán, G., Chen, G., Tsuchiya, E., Wilson, L., Jordan, M. A., & Sikic, B. I. (1995) *Oncol. Res. 7*, 517−527.

Jordan, M. A., Thrower, D., & Wilson, L. (1991) *Cancer Res. 51*, 2212−2222.

Jordan, M. A., Toso, R. J., Thrower, D., & Wilson, L. (1993) *Proc. Natl. Acad. Sci. U.S.A. 90*, 9552−9556.

Jordan, M. A., Wendell, K., Gardiner, S., Derry, W. B., Copp, H., & Wilson, L. (1996) *Cancer Res. 56*, 816−825.

Khan, I. A., & Ludueña, R. F. (1996) *Biochemistry 35*, 3704−3711.

Kowalski, R. J., & Williams, R. C. (1993) *Cell Motil. Cytoskel. 26*, 282−290.

Kumar, N. (1981) *J. Biol. Chem. 256*, 10435−10441.

Lewis, S. A., Gu, W., & Cowan, N. J. (1987) *Cell 49*, 539−548.

Lobert, S., Frankfurter, A., & Correia, J. J. (1995) *Biochemistry 34*, 8050−8060.

Lopata, M. A., & Cleveland, D. W. (1987) *J. Cell Biol. 105*, 1707−1720.

Lu, Q., & Ludueña, R. F. (1993) *Cell Struct. Funct. 18*, 173−182.

Lu, Q., & Ludueña, R. F. (1994) *J. Biol. Chem. 269*, 2041−2047.

Ludueña, R. F. (1993) *Mol. Biol. Cell 4*, 445−457.

Margolis, R. L., & Wilson, L. (1978) *Cell 8*, 1−13.

Matthews, K. A., Rees, D., & Kaufman, T. C. (1993) *Development 117*, 977−991.

McGuire, W. P., Hoskins, W. J., Brady, M. F., Kucera, P. R., Partridge, E. E., Look, K. Y., Clarke-Pearson, D. L., & Davidson, M. (1996) *N. Engl. J. Med. 334*, 1−6.

Minotti, A. M., Barlow, S. B., & Cabral, F. (1991) *J. Biol. Chem. 266*, 3987−3994.

Mitchison, T. J., & Kirschner, M. (1984a) *Nature 312*, 232−237.

Mitchison, T. J., & Kirschner, M. (1984b) *Nature 312*, 237−242.

Ohta, S., Nishio, K., Kubota, N., Ohmori, T., Funayama, Y., Ohira, T., Nakajima, H., Adachi, M., & Saijo, N. (1994) *Jpn. J. Cancer Res. 85*, 290−297.

Panda, D., Miller, H. P., Banerjee, A., Ludueña, R. F., & Wilson, L. (1994) *Proc. Natl. Acad. Sci. U.S.A. 91*, 11358−11362.

Panda, D., Goode, B. L., Feinstein, S. C., & Wilson, L. (1995) *Biochemistry 34*, 11117−11127.

Parness, J., & Horwitz, S. B. (1981) *J. Cell Biol. 91*, 479−487.

Pryer, N. K., Walker, R. A., Skeen, V. P., Bourns, B. D., Soboeiro, M. F., & Salmon, E.D. (1992) *J. Cell Sci. 103*, 965−976.

Ranganathan, S., Dexter, D. W., Benetatos, C. A., Chapman, A. E., Tew, K. D., & Hudes, G. R. (1996) *Cancer Res. 56*, 2584−2589.

Rao, S., Krauss, N. E., Heerding, J. M., Swindell, C. S., Ringel, I., Orr, G. A., & Horwitz, S. B. (1994) *J. Biol. Chem. 269*, 3132−3134.

Rao, S., Orr, G. A., Chaudhary, A. G., Kingston, D. G. I., & Horwitz, S. B. (1995) *J. Biol. Chem. 270*, 20235−20238.

Rowinski, E. K., Donehower, R. C., Jones, R. J., & Tucker, R. W. (1988) *Cancer Res. 49*, 4093−4100.

Roy, S. N., & Horwitz, S. B. (1985) *Cancer Res. 45*, 3856−3863.

Schibler, M. J. & Cabral, F. (1986) *J. Cell Biol. 102*, 1522−1531.

Schiff, P. B., & Horwitz, S. B. (1980) *Proc. Natl. Acad. Sci. U.S.A. 77*, 1561−1565.

Schiff, P. B., Fant, J., & Horwitz, S. B. (1979) *Nature 277*, 665−667.

Sullivan, K. F. (1988) *Ann. Rev. Cell Biol. 4*, 687−716.

Toso, R. J., Jordan, M. A., Farrell, K. W., Matsumoto, B., & Wilson, L. (1993) *Biochemistry 32*, 1285−1293.

Walker, R. A., O'Brien, E. T., Pryer, N. K., Soboeiro, M. F., Voter, W. A., Erickson, H. P., & Salmon, E. D. (1988) *J. Cell Biol. 107*, 1437−1448.

Wilson, L., Miller, H. P., Farrell, K. W., Snyder, K. B., Thompson, W. C., & Purich, D. L. (1985) *Biochemistry 24*, 5254−5262.

BI962724M